J. Fluid Mech. (2015), *vol.* 772, *pp.* 740–755. © Cambridge University Press 2015
doi:10.1017/jfm.2015.229

Equilibrium similarity solution of the turbulent transport equation along the centreline of a round jet

H. Sadeghi[1], P. Lavoie[1,†] and A. Pollard[2]

[1]Institute for Aerospace Studies, University of Toronto, Toronto, ON, M3H 5T6, Canada

[2]Department of Mechanical and Materials Engineering, Queen's University, Kingston, ON, K7L 3N6, Canada

(Received 21 August 2014; revised 14 February 2015; accepted 16 April 2015; first published online 8 May 2015)

A novel similarity-based form is derived of the transport equation for the second-order velocity structure function of $\langle(\delta q)^2\rangle$ along the centreline of a round turbulent jet using an equilibrium similarity analysis. This self-similar equation has the advantage of requiring less extensive measurements to calculate the inhomogeneous (decay and production) terms of the transport equation. It is suggested that the normalised third-order structure function can be uniquely determined when the normalised second-order structure function, the power-law exponent of $\langle q^2\rangle$ and the decay rate constants of $\langle u^2\rangle$ and $\langle v^2\rangle$ are available. In addition, the current analysis demonstrates that the assumption of similarity, combined with an inverse relation between the mean velocity U and the streamwise distance $x - x_0$ from the virtual origin (i.e. $U \propto (x - x_0)^{-1}$), is sufficient to predict a power-law decay for the turbulence kinetic energy ($\langle q^2\rangle \propto (x - x_0)^m$), rather than requiring a power-law decay ($m = -2$) as an additional *ad hoc* assumption. On the basis of the current analysis, it is suggested that the mean kinetic energy dissipation rate, $\langle\epsilon\rangle$, varies as $(x - x_0)^{m-2}$. These theoretical results are tested against new experimental data obtained along the centreline of a round turbulent jet as well as previously published data on round jets for $11\,000 \leqslant Re_D \leqslant 184\,000$ over the range $10 \leqslant x/D \leqslant 90$. For the present experiments, $\langle q^2\rangle$ exhibits power-law behaviour with $m = -1.83$. The validity of this solution is confirmed using other experimental data where $\langle q^2\rangle$ follows a power law with $-1.89 \leqslant m \leqslant -1.78$. The present similarity form of the transport equation for $\langle(\delta q)^2\rangle$ is also shown to be closely satisfied by the experimental data.

Key words: jets, turbulence theory, turbulent flows

1. Introduction

The concept of similarity, or self-preservation, which assumes that the flow scales with single velocity and length scales, has been an important tool for analysis in turbulence research. One major benefit of this concept is the reduction of the number of equations that may be used to describe turbulent flows. The similarity of the mean

† Email address for correspondence: lavoie@utias.utoronto.ca

momentum and turbulent energy equations for jet flows has been discussed extensively in many papers (e.g. Panchapakesan & Lumley 1993; Burattini, Antonia & Danaila 2005*b*) and textbooks (e.g. Tennekes & Lumley 1972; Pope 2000). For turbulent round jets, an empirical observation is that the profiles of $U_m/U(x)$ and $\langle u_i u_j\rangle/U(x)^2$ become self-similar (i.e. independent of the downstream location of the jet, x) when expressed in terms of $\xi \equiv y/y_{0.5}(x)$; here U_m is the mean streamwise velocity, $U(x)$ is the axial velocity along the jet centreline, and $\langle u_i u_j\rangle$ is the Reynolds shear stress. The parameter $\xi \equiv y/y_{0.5}(x)$ is the similarity variable, where y is the radial coordinate and $y_{0.5}$ is the jet half-width radius, which is defined as the radial location at which the mean jet velocity is equal to half the local maximum mean velocity relative to the centreline. Experimental evidence has shown that $y_{0.5} = S(x - x_0)$, where S is the spread rate of the jet and x_0 is the virtual origin, which depends on the initial conditions (George 1989; Malmstrom *et al.* 1997; Fellouah, Ball & Pollard 2009). Based on the classical self-similarity concept in round jets, the outer turbulent length scale grows approximately linearly along the centreline (e.g. $\ell \propto (x - x_0)$, where ℓ is a typical outer length scale), and the mean velocity is inversely proportional to distance ($U \propto (x - x_0)^{-1}$). Assuming that the normalised mean kinetic energy dissipation rate parameter is constant ($C_\epsilon = \langle\epsilon\rangle\ell/u_0^{3/2}$, with u_0 being a typical turbulent velocity scale and assumed to vary as $(x - x_0)^{-2}$), it can be obtained that the mean kinetic energy dissipation rate, $\langle\epsilon\rangle$, varies as $(x - x_0)^{-4}$ (e.g. Antonia, Satyaprakash & Hussain 1980). It has also been documented for some time that the turbulence intensity ($\langle u^2\rangle^{0.5}/U$) reaches a plateau when the jet is self-similar. Given the fact that U is inversely proportional to distance, $\langle u^2\rangle$ therefore has to follow a power law along the centreline with an exponent equal to -2. In Tennekes & Lumley (1972), it was noted that turbulence intensities are about half an order of magnitude smaller than the jet velocity if Re is infinite and $y_{0.5}/x \to 0$. However, these assumptions are not realised in turbulent flows encountered in laboratory conditions, where both Re and x are finite. In addition, the effect of initial conditions on the power-law behaviour of turbulent kinetic energy was ignored. A key aim of this paper is to demonstrate that these assumptions can be relaxed significantly and that the form of the streamwise evolution of the velocity fluctuations and dissipation, as well as their decay, can be obtained directly from the governing equations.

The concept of similarity has been not only applied to the mean momentum and turbulent energy equations but also investigated for all scales of motion. George (1992) (referred to as G92 hereafter) applied his analysis (known as equilibrium similarity) to the decay of homogeneous, isotropic turbulence by considering the spectral energy equation

$$\frac{\partial E(k)}{\partial t} = T(k) - 2\nu k^2 E(k), \tag{1.1}$$

where $E(k)$ is the three-dimensional kinetic energy spectrum and $T(k)$ is the nonlinear spectral transfer function. G92 showed that all terms in (1.1) evolve in exactly the same manner, with the mean turbulent kinetic energy $\langle q^2\rangle = \langle u^2\rangle + \langle v^2\rangle + \langle w^2\rangle$ and the Taylor microscale λ used as appropriate scaling parameters to normalise all scales of motion. In addition, it was shown that $\langle q^2\rangle$ decays as a power law in time, and that λ grows as the square root of time. The coefficient and decay rate in the power-law equation of $\langle q^2\rangle$ were shown to be dependent on initial conditions.

In addition to the spectral energy equation, the transport equation for the second-order structure function has received particular attention. Burattini, Antonia & Danaila (2005*a*) derived a transport equation for the total turbulent energy structure function $\langle(\delta q)^2\rangle$ ($= \langle(\delta u)^2\rangle + \langle(\delta v)^2\rangle + \langle(\delta w)^2\rangle$) from the incompressible Navier–Stokes

equations along the centreline of a turbulent round jet using the same procedure as in Danaila *et al.* (2001) and Danaila, Anselmet & Antonia (2002), *viz.*

$$-\langle(\delta u)(\delta q)^2\rangle + 2\nu\frac{\mathrm{d}}{\mathrm{d}r}\langle(\delta q)^2\rangle - \frac{U}{r^2}\int_0^r s^2\frac{\partial}{\partial x}\langle(\delta q)^2\rangle\,\mathrm{d}s$$
$$-2\frac{\partial U}{\partial x}\frac{1}{r^2}\int_0^r s^2(\langle(\delta u)^2\rangle - \langle(\delta v)^2\rangle)\,\mathrm{d}s = \frac{4}{3}\langle\epsilon\rangle r. \tag{1.2}$$

In this equation, $\delta u \equiv u(x+r) - u(x)$ is the longitudinal velocity increment (for the streamwise velocity component u), r is the distance between two points considered along the x direction, U is the mean streamwise velocity along the centreline, s is a dummy separation variable, and $\langle(\delta u)^2\rangle$, $\langle(\delta v)^2\rangle$ and $\langle(\delta w)^2\rangle$ are the second-order structure functions of u, v and w, respectively. The first term on the left-hand side of (1.2) is the third-order structure function that represents advection, while the second term is diffusion, which represents viscous effects. The third term quantifies the role of the streamwise inhomogeneity. The fourth term represents the role of the energy production. The right-hand side of (1.2) is proportional to the mean dissipation rate of turbulent kinetic energy and balances the sum of the terms on the left-hand side. In Burattini *et al.* (2005*a*), (1.2) was satisfied along the centreline of a round jet ($35 \leqslant x/D \leqslant 90$) by the hot-wire data to an acceptable approximation. It was shown that although the sum of the advection and diffusion terms balances dissipation at small scales, inclusion of the production and streamwise inhomogeneity terms leads to a satisfactory balance for the whole range of scales. However, computation of the streamwise inhomogeneity term requires $\langle(\delta q)^2\rangle$ to be known at different streamwise locations, which involves significant uncertainties associated with numerical differentiation of the data. This may lead to an imbalance between the dissipation and the terms on the left-hand side of (1.2). As will be discussed later, this issue can be resolved significantly by using a similarity approach such as the one proposed here. Burattini *et al.* (2005*a*,*b*) were the first to consider a similarity analysis of the transport equation for the centreline of a round jet. Burattini *et al.* (2005*b*) suggested that self-similar forms can exist for each term of (1.2) independent of the Reynolds number and the choice of similarity variables. They also showed experimentally that the energy structure functions, measured at a number of locations along the axis of the jet, collapse over a significant range of scales when normalised by λ (as well as the Kolmogorov scale, η, and the integral scale, L) and $\langle q^2\rangle$.

In the present work, we extend the equilibrium similarity analysis of G92 to the turbulent energy structure function in a round turbulent jet, i.e. (1.2). Based on our analysis, the similarity variables are formally obtained from the governing equations. One major consequence of the current analysis is that new forms of the decay law of velocity fluctuations and dissipation are obtained with no further assumptions (or empirical observations) on the characteristic length and velocity scales. Finally, a novel self-similar form of (1.2) is derived. A particularly useful feature of the current analysis is that it can alleviate some of the difficulties involved in calculating the $\partial/\partial x$ terms (production and decay terms). As will be demonstrated, the terms in the energy scale budget equation can be studied if $\langle(\delta q)^2\rangle$ and the mean velocity are measured at a single point. This avoids the necessity of measuring the structure functions at different axial locations and the related uncertainties associated with the numerical differentiation (Lavoie *et al.* 2005; Antonia & Burattini 2006). It should be mentioned that the present equilibrium similarity solution does not require the Reynolds number

to be large for a specified set of initial conditions (George 1992). The suggested similarity solutions are tested against new experimental data and previously reported data, which were all taken along the centreline of a round jet.

2. Theoretical considerations

In order to bring (1.2) into a self-similar form, following Antonia *et al.* (2003), Burattini *et al.* (2005*b*) and G92, we assume that

$$\langle(\delta q)^2\rangle = Q(x)f(\tilde{r}), \tag{2.1}$$

$$\langle(\delta u)^2\rangle = M(x)e(\tilde{r}), \tag{2.2}$$

$$\langle(\delta v)^2\rangle = R(x)h(\tilde{r}), \tag{2.3}$$

$$-\langle(\delta u)(\delta q)^2\rangle = T(x)g(\tilde{r}), \tag{2.4}$$

where $Q(x)$, $M(x)$ and $R(x)$ are velocity scales that characterise the second-order structure functions of q, u and v, and $T(x)$ characterises the third-order structure function $-\langle(\delta u)(\delta q)^2\rangle$. Here $\tilde{r} = r/\ell$, where r is the streamwise separation and ℓ is a characteristic length scale which is to be determined.

Upon substituting (2.1)–(2.4) into (1.2), differentiating, rearranging terms by separating terms that depend on x from those that depend on r/ℓ and multiplying by $\ell/(\nu Q(x))$, we obtain

$$\left[\frac{T(x)\ell}{\nu Q(x)}\right] g + [2]\frac{\mathrm{d}f}{\mathrm{d}\tilde{r}} + \left[\frac{U\ell}{\nu}\frac{\mathrm{d}\ell}{\mathrm{d}x}\right]\frac{\Gamma_1}{\tilde{r}^2} - \left[\frac{U\ell^2}{\nu Q(x)}\frac{\mathrm{d}Q(x)}{\mathrm{d}x}\right]\frac{\Gamma_2}{\tilde{r}^2} - \left[2\frac{\mathrm{d}U}{\mathrm{d}x}\frac{M(x)}{\nu Q(x)}\ell^2\right]\frac{\Gamma_3}{\tilde{r}^2} + \left[2\frac{\mathrm{d}U}{\mathrm{d}x}\frac{R(x)}{\nu Q(x)}\ell^2\right]\frac{\Gamma_4}{\tilde{r}^2} = \frac{4}{3}\left[\frac{\langle\epsilon\rangle\ell^2}{\nu Q(x)}\right]\tilde{r}, \tag{2.5}$$

where

$$\Gamma_1 = \int_0^{r/\ell}\left(\frac{s}{\ell}\right)^3\frac{\mathrm{d}f}{\mathrm{d}\tilde{r}}\,\mathrm{d}\left(\frac{s}{\ell}\right), \quad \Gamma_2 = \int_0^{r/\ell}\left(\frac{s}{\ell}\right)^2 f\,\mathrm{d}\left(\frac{s}{\ell}\right), \tag{2.6a,b}$$

$$\Gamma_3 = \int_0^{r/\ell}\left(\frac{s}{\ell}\right)^2 e\,\mathrm{d}\left(\frac{s}{\ell}\right), \quad \Gamma_4 = \int_0^{r/\ell}\left(\frac{s}{\ell}\right)^2 h\,\mathrm{d}\left(\frac{s}{\ell}\right). \tag{2.7a,b}$$

Since the multiplier in the second term of (2.5) is constant, all the other terms must also be constant for similarity to hold. They can be rewritten as

$$\left[\frac{T(x)\ell}{\nu Q(x)}\right] = \text{constant}, \tag{2.8}$$

$$\left[\frac{U\ell}{\nu}\frac{\mathrm{d}\ell}{\mathrm{d}x}\right] = a, \tag{2.9}$$

$$\left[\frac{U\ell^2}{\nu Q(x)}\frac{\mathrm{d}Q(x)}{\mathrm{d}x}\right] = b, \tag{2.10}$$

$$\left[2\frac{\mathrm{d}U}{\mathrm{d}x}\frac{M(x)}{\nu Q(x)}\ell^2\right] = c, \tag{2.11}$$

$$\left[2\frac{\mathrm{d}U}{\mathrm{d}x}\frac{R(x)}{\nu Q(x)}\ell^2\right] = d, \tag{2.12}$$

$$\left[\frac{\langle\epsilon\rangle\ell^2}{\nu Q(x)}\right] = \text{constant}. \tag{2.13}$$

In order to calculate all the constants, some additional information is required. As the momentum flux is constant, the velocity along the centreline of a round jet can be obtained as (see Pope 2000)

$$U = C/(x - x_0), \tag{2.14}$$

where C is a constant and x_0 is the virtual origin. For the region near the axisymmetric jet centreline, the kinetic energy budget equation can be approximated as (see Burattini *et al.* 2005*a*)

$$\langle\epsilon\rangle = -\frac{U}{2}\frac{\mathrm{d}\langle q^2\rangle}{\mathrm{d}x} - (\langle u^2\rangle - \langle v^2\rangle)\frac{\mathrm{d}U}{\mathrm{d}x}, \tag{2.15}$$

where

$$\langle q^2\rangle = \langle u^2\rangle + 2\langle v^2\rangle. \tag{2.16}$$

Substituting (2.15) into (2.13) and multiplying by a factor of -2 gives

$$\left[\frac{U}{\nu Q(x)}\frac{\mathrm{d}\langle q^2\rangle}{\mathrm{d}x}\ell^2\right] + \left[2\frac{\mathrm{d}U}{\mathrm{d}x}\frac{(\langle u^2\rangle - \langle v^2\rangle)}{\nu Q(x)}\ell^2\right] = \text{constant}. \tag{2.17}$$

Subtracting (2.12) from (2.11) yields

$$\left[2\frac{\mathrm{d}U}{\mathrm{d}x}\frac{M(x) - R(x)}{\nu Q(x)}\ell^2\right] = \text{constant}. \tag{2.18}$$

If (2.10) is added to (2.18), then

$$\left[\frac{U}{\nu Q(x)}\frac{\mathrm{d}Q(x)}{\mathrm{d}x}\ell^2\right] + \left[2\frac{\mathrm{d}U}{\mathrm{d}x}\frac{M(x) - R(x)}{\nu Q(x)}\ell^2\right] = \text{constant}. \tag{2.19}$$

Comparing (2.19) with (2.17), it follows that $Q(x) \sim \langle q^2\rangle$ and $M(x) - R(x) \sim \langle u^2\rangle - \langle v^2\rangle$. Here, $M(x)$ and $R(x)$ may be related to the velocity fluctuations $\langle u^2\rangle$ and $\langle v^2\rangle$, respectively.

Integration of (2.9) yields

$$\ell^2 = \frac{a}{C}\nu(x - x_0)^2, \tag{2.20}$$

which indicates that the characteristic length scales linearly with $(x - x_0)$. Using (2.14) and the fact that $Q(x) \sim \langle q^2\rangle$, (2.10) can be written as

$$\left[\frac{C\ell^2}{\nu(x - x_0)}\frac{\mathrm{d}\langle q^2\rangle}{\langle q^2\rangle}\frac{1}{\mathrm{d}x}\right] = b. \tag{2.21}$$

Upon substituting (2.20) into (2.21) and performing some simplifications, it emerges that

$$\frac{\mathrm{d}\langle q^2\rangle}{\langle q^2\rangle} = \frac{b}{a}\frac{\mathrm{d}x}{(x - x_0)}. \tag{2.22}$$

The solution of (2.22) takes the form

$$\langle q^2\rangle = A(x-x_0)^m, \tag{2.23}$$

where $m = b/a$. This equation indicates that the characteristic velocity scale should follow a power law along the jet centreline. Comparing (2.11) and (2.12) suggests that

$$\frac{M(x)}{R(x)} = \frac{\langle u^2\rangle}{\langle v^2\rangle} \tag{2.24}$$

remains constant. Therefore, by considering (2.16) and (2.23), it follows that

$$\langle u^2\rangle = A_1(x-x_0)^m, \tag{2.25}$$

$$\langle v^2\rangle = A_2(x-x_0)^m \tag{2.26}$$

and $A = A_1 + 2A_2$. Substituting (2.14), (2.23), (2.25) and (2.26) into (2.15) gives

$$\langle\epsilon\rangle = C\left[\frac{-(A_1+2A_2)m}{2} + (A_1 - A_2)\right](x-x_0)^{m-2}. \tag{2.27}$$

From (2.27) it immediately follows that the dissipation $\langle\epsilon\rangle$ decays with an exponent of $m-2$ along the centreline. Substituting (2.23) and (2.27) into the general equation for the Taylor microscale (Antonia *et al.* 2003), *viz.*

$$\lambda^2 = 5\nu\frac{\langle q^2\rangle}{\langle\epsilon\rangle}, \tag{2.28}$$

gives

$$\lambda^2 = 5\nu\frac{2(A_1+2A_2)}{-C(A_1+2A_2)m + 2C(A_1-A_2)}(x-x_0)^2. \tag{2.29}$$

Comparing (2.20) and (2.29) confirms that λ is the relevant characteristic length scale (i.e. $\ell = \lambda$). With $\ell = \lambda$ and $Q(x) \sim \langle q^2\rangle$, (2.8) implies that

$$T(x) \sim \nu\frac{\langle q^2\rangle}{\lambda}, \tag{2.30}$$

or

$$T(x) \sim Re_\lambda^{-1}\langle q^2\rangle^{3/2}, \tag{2.31}$$

where the corresponding turbulence Reynolds number is defined here as (cf. Antonia *et al.* 2003)

$$Re_\lambda = \frac{\langle q^2\rangle^{1/2}\lambda}{3^{1/2}\,\nu}. \tag{2.32}$$

By considering $Q(x) \equiv \langle q^2\rangle$ and $T(x) \equiv 3^{-1/2}Re_\lambda^{-1}\langle q^2\rangle^{3/2}$ and performing some manipulations, (2.5) can be written as

$$g + 2\frac{\mathrm{d}f}{\mathrm{d}\tilde{r}} + 10(c_1+2c_2)\frac{\Gamma_1}{\tilde{r}^2} - 10m(c_1+2c_2)\frac{\Gamma_2}{\tilde{r}^2} + 20c_1\frac{\Gamma_3}{\tilde{r}^2} - 20c_2\frac{\Gamma_4}{\tilde{r}^2} = \frac{20}{3}\tilde{r}, \tag{2.33}$$

where

$$c_1 = \frac{A_1}{-(A_1+2A_2)m + 2(A_1-A_2)}, \quad c_2 = \frac{A_2}{-(A_1+2A_2)m + 2(A_1-A_2)}. \tag{2.34a,b}$$

The normalised form of the third-order structure function g can be determined when the normalised second-order structure function f, the power-law exponent m of $\langle q^2 \rangle$ and the decay rate constants A_1 and A_2 are known. A particularly useful feature of this self-similar equation is that it avoids the difficulties involved in calculating the $\partial/\partial x$ terms (production and decay terms) in (1.2).

For simplicity, (2.33) can be rewritten as

$$A + B + D + P = C, \tag{2.35}$$

where A is the turbulent advection term (the generalised third-order structure function or the first term on the left-hand side of (2.33)), B is the diffusion term (second term on the left-hand side of (2.33)), D is the inhomogeneous decay term along the streamwise direction x (the sum of the third and fourth terms on the left-hand side of (2.33)), P is the production term (the sum of the fifth and sixth terms on the left-hand side of (2.33)) and C is the dissipation term and the balance of all the other terms (the right-hand side term in (2.33)).

3. Experimental details

Experimental measurements were performed to test the similarity solutions obtained in the previous section. An air jet was generated using a fan mounted on antivibration pads. The air then exits a settling chamber via a round duct to the inlet of a smoothly contracting axisymmetric nozzle. The experiments were carried out at the exit Reynolds number of $Re_D = 50\,000$, where Re_D is calculated based on the jet exit mean velocity ($U_j = 10.65$ m s^{-1}) and the nozzle exit diameter $D = 0.0736$ m. The jet has a top-hat velocity profile at the exit. The axial turbulence intensity in the potential core of the flow near the jet exit was less than 0.7 % (see Sadeghi & Pollard 2012 and Sadeghi, Lavoie & Pollard 2014 for further details about the exit conditions of the jet). The measurements were performed for $10 \leqslant x/D \leqslant 25$. Measurements of the turbulence statistics were obtained using a stationary cross-wire probe. The wires were made of 2.5 μm diameter tungsten wire with a 0.5 mm sensing length. The hot-wires were calibrated in the jet core before and after each experiment. Similar to the scheme described in Burattini & Antonia (2005), the cross-wire was calibrated using a look-up table, with calibration angles within the range ±40°, in intervals of 10°. The signals were low-pass filtered at a cutoff frequency f_c, which was selected based on the onset of electronic noise and close to the Kolmogorov frequency, $f_k \equiv U/2\pi\eta$, where $\eta \equiv \nu^{3/4}/\langle\epsilon\rangle^{1/4}$. The measurements were taken with a sampling frequency of $f_s \geqslant 2f_c$. The sampling time was selected to ensure that enough data would be taken to achieve statistical convergence of $\langle q^2 \rangle$ (at least within ±2 %) and in the peak value of the generalised normalised third-order structure function $\langle(\delta u)^2(\delta q)\rangle$ (at least within ±4 %, which typically required 10 min of sampling time). In the present work, the modified Taylor hypothesis based on the models developed by Lumley (1965) was used to convert time into a spatial series. In addition, data were corrected for the effect of high-frequency noise and finite spatial resolution (Hearst *et al.* 2012; Xu *et al.* 2013; Sadeghi *et al.* 2014).

Characterisation of the small-scale motions in turbulent flows has been a challenging problem in turbulence research, especially in turbulent shear flows. One of the primary experimental concerns has been the determination of the mean-square gradients of the fluctuating velocity field to estimate the rate of dissipation of turbulence kinetic energy, *viz.*

$$\langle\epsilon\rangle = \frac{1}{2}\nu\left\langle\left(\frac{\partial u_i}{\partial x_j} + \frac{\partial u_j}{\partial x_i}\right)^2\right\rangle. \tag{3.1}$$

Twelve separate derivative correlations must be determined before the dissipation can be truly calculated. Since it is difficult to calculate all velocity derivatives accurately from experimental measurements, it has been common to use alternative assumptions to estimate the dissipation rate. The most well-known assumption is local isotropy. The dissipation for isotropic turbulence reduces to

$$\langle \epsilon \rangle_{iso} = 15\nu \left\langle \left(\frac{\partial u}{\partial x} \right)^2 \right\rangle. \tag{3.2}$$

This is the simplest definition of the dissipation, which has been extensively used to estimate the dissipation rate in experimental studies, even when the flow was not exactly locally isotropic. The failure of local isotropy in turbulent jet flows has long been documented in the literature (e.g. Wygnanski & Fiedler 1969; Champagne 1978; Burattini & Antonia 2005; Burattini *et al.* 2005*b*). Using homogeneity and incompressibility, another estimate for the dissipation can be obtained as (see e.g. Hinze 1975; George & Hussein 1991)

$$\langle \epsilon \rangle_{hom} = \nu \left\langle \left(\frac{\partial u_i}{\partial x_j} \right)^2 \right\rangle. \tag{3.3}$$

By assuming axisymmetry, a relatively crude approximation for this equation can be obtained as (e.g. Danaila *et al.* 2002; Burattini *et al.* 2005*a*,*b*)

$$\langle \epsilon \rangle_{hom} = 3\nu \left[\left\langle \left(\frac{\partial u}{\partial x} \right)^2 \right\rangle + 2 \left\langle \left(\frac{\partial v}{\partial x} \right)^2 \right\rangle \right]. \tag{3.4}$$

The components for estimating the dissipation from (3.4) can be obtained with a cross-wire. Following previous studies in jet flows (e.g. Burattini *et al.* 2005*a*,*b*), $\langle \epsilon \rangle_{hom}$ is used here as the dissipation since the assumptions employed for its estimate are less restrictive than the alternative assumption of local isotropy along the jet centreline.

Table 1 provides estimates of several parameters measured downstream of the current jet, including the dissipation estimated with the aforementioned techniques. Using the dissipation and longitudinal integral scale (L_u), the non-dimensional energy dissipation rate, C_ϵ, along the centreline of the jet is also listed in table 1. Here, C_ϵ is defined as

$$C_\epsilon \equiv L_u \langle \epsilon \rangle \langle u^2 \rangle^{-3/2}, \tag{3.5}$$

where

$$L_u = \frac{1}{\langle u^2 \rangle} \int_0^{r_0} B_{u,u}(r)\, \mathrm{d}r, \tag{3.6}$$

with $B_{u,u}$ being the correlation of $\langle \alpha(x+r)\alpha(x) \rangle$.

The dissipation (or the mean-square gradients of the fluctuating velocity field) can be used to estimate other important turbulent length scales (i.e. the Taylor microscale, λ, and the Kolmogorov length scale, η). The Taylor microscale and the Taylor Reynolds number have been extensively estimated in the literature using the isotropic relations of

$$\lambda_{iso} = \frac{\langle u^2 \rangle^{1/2}}{\left\langle \left(\frac{\partial u}{\partial x} \right)^2 \right\rangle^{1/2}} \tag{3.7}$$

x/D	10	15	20	25	
$\langle\epsilon\rangle_{iso}$	37	13.01	5.63	3	(m^2 s^{-3})
$\langle\epsilon\rangle_{hom}$	33.86	9.30	3.39	1.68	(m^2 s^{-3})
λ_{iso}	3.45	4.21	4.98	5.81	mm
λ_{hom}	3.16	4.36	5.64	6.73	mm
$Re_{\lambda_{iso}}$	302	265	245	243	
$Re_{\lambda_{hom}}$	242	242	243	244	
η_{iso}	0.101	0.131	0.162	0.189	mm
η_{hom}	0.103	0.143	0.184	0.219	mm
L_u	40	54	70	86	mm
$C_{\epsilon_{hom}}$	0.53	0.52	0.52	0.51	

TABLE 1. Turbulent flow properties at four downstream locations along the jet centreline.

and

$$Re_{\lambda_{iso}} = \frac{\langle u^2\rangle^{1/2}\lambda_{iso}}{\nu}, \tag{3.8}$$

respectively. However, in the current work, more general definitions of Taylor microscale, (2.28), and Taylor microscale Reynolds number, (2.32), which avoid the directional ambiguity of the turbulence statistics, are used (Corrsin 1963; Fulachier & Antonia 1983; Antonia *et al.* 2003). In table 1, λ_{hom} and $Re_{\lambda_{hom}}$ are estimated by using $\langle\epsilon\rangle_{hom}$ in (2.28) and (2.32). The Kolmogorov length scale of η_{hom} is obtained by substituting $\langle\epsilon\rangle_{hom}$ into

$$\eta \equiv \nu^{3/4}/\langle\epsilon\rangle^{1/4}. \tag{3.9}$$

The values for λ_{iso}, $Re_{\lambda_{iso}}$ and η_{iso} are also provided for reference as they are the most common parameters cited in many other works.

4. Presentation and discussion of the experimental results

The similarity of the mean momentum equations is investigated over the present range of measurements. For this purpose, the radial profiles of the mean velocity and Reynolds shear stress are presented for four locations ($x/D = 10$, 15, 20 and 25) in figure 1. The profiles are normalised by the jet half-velocity radius ($y_{0.5}$) and the mean centreline velocity (U_c), which are the relevant scales for the self-similarity of mean momentum equations in jet flows (see e.g. Pope 2000; Burattini *et al.* 2005*b*). The profiles of the mean velocity and Reynolds shear stress exhibit satisfactory collapse over the present range of measurements.

The axial mean velocity along the jet centreline is displayed in figure 2. As expected, it decays almost linearly with axial distance. For a self-similar jet, the centreline velocity variation can be written as

$$\frac{U_j}{U_c} = \frac{1}{B}\left(\frac{x - x_0}{D}\right), \tag{4.1}$$

which is the inverted normalised form of (2.14). A least-squares fit to the data gives a mean velocity decay constant of $B = 6.6$ (or $C = B * D * U_j = 5.17$) and a virtual origin of $x_0 = -1.68D$. Here, B is very similar to the values obtained by Weisgraber & Liepman (1998) and Ferdman, Otugen & Kim (2000) ($B \sim 6.7$) and is in good

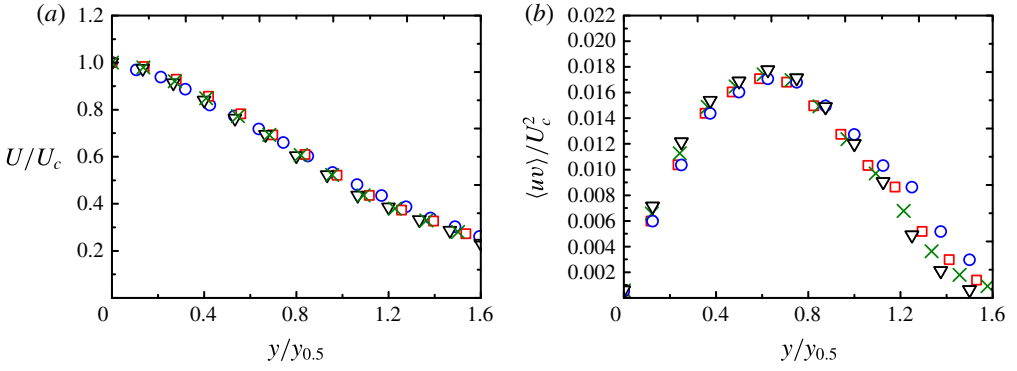

FIGURE 1. (Colour online) Radial profiles of (*a*) mean velocity and (*b*) Reynolds shear stress at four axial locations: ○, $x/D = 10$; □, $x/D = 15$; ▽, $x/D = 20$; ×, $x/D = 25$.

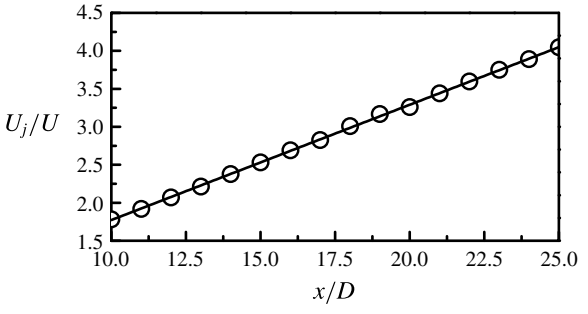

FIGURE 2. Axial decay of the mean velocity along the centreline; the solid line is the least-squares fit to the data.

agreement with the results of Panchapakesan & Lumley (1993) and Burattini *et al.* (2005*b*) ($B \sim 6.1$). It is generally accepted that there will be some variability in the mean velocity decay constant and virtual origin (see e.g. table 1 in Fellouah *et al.* 2009) for different experiments, which is typically related to differences in the measurement region, exit Reynolds number, experimental technique and initial conditions (Malmstrom *et al.* 1997; Xu & Antonia 2002; Pollard & Uddin 2007).

The streamwise variations of $\langle q^2\rangle$, $\langle u^2\rangle$ and $\langle v^2\rangle$, measured along the jet centreline and normalised by U_j^2, are shown in figure 3(*a*). A curve fit was applied to the data using the virtual origin of $x_0 = -1.68D$. It was found that $\langle q^2\rangle$, $\langle u^2\rangle$ and $\langle v^2\rangle$ follow closely a power law with exponent $m = -1.83$, in agreement with (2.23)–(2.26). The decay rate constants for $\langle q^2\rangle$, $\langle u^2\rangle$ and $\langle v^2\rangle$ are estimated to be $A = 3.29$, $A_1 = 1.43$ and $A_2 = 0.93$, respectively. In order to investigate the validity of the solution over an extended streamwise range, we have tested the equilibrium similarity solution using three previously published experimental datasets, where data have been taken over a longer streamwise distance. The evolution of $\langle q^2\rangle$ ($\equiv \langle u^2\rangle + 2\langle v^2\rangle$) along the centreline of axisymmetric turbulent jets from previous studies is illustrated in figure 3(*b*). The experimental conditions for these studies are summarised in table 2. Curve fits were applied to the data using the corresponding virtual origins listed in table 2. It was found that in the aforementioned experiments, $\langle q^2\rangle$ follows a power law with $-1.89 \leqslant m \leqslant -1.78$, consistent with the present data. As both downstream

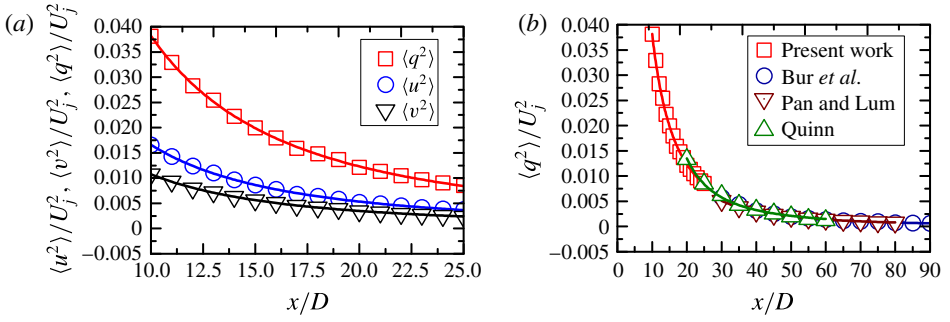

FIGURE 3. (Colour online) (*a*) Streamwise variation of normalised $\langle q^2\rangle$ (□), $\langle u^2\rangle$ (○) and $\langle v^2\rangle$ (△) along the centreline of the current jet. (*b*) Streamwise variation of normalised $\langle q^2\rangle$ along the centreline of round jets: ▽, from Panchapakesan & Lumley (1993); ○, from Burattini *et al.* (2005*b*); △, from Quinn (2006); □, from the current work. The solid lines represent least-squares fits to the data.

Authors	D (mm)	U_j (m s^{-1})	Re_D	x_0/D	x/D	m
Panchapakesan & Lumley (1993)	6.1	27	11 000	0	30–80	−1.89
Burattini *et al.* (2005*b*)	55	35.1	140 000	4.40	30–90	−1.84
Quinn (2006)	45.3	61	184 000	3.65	20–60	−1.78

TABLE 2. Experimental conditions on the jet centreline for different round jets.

distance and Reynolds number are finite in previous experiments as well as in the current work, it is not unexpected to observe that the exponent for $\langle q^2\rangle$ (or $\langle u^2\rangle$) is not the traditional value of -2 but rather a slightly greater value. In addition, the influence on m of measurement uncertainties and slight differences in initial conditions cannot be ignored. Assuming $\langle u^2\rangle \sim (x-x_0)^m$ and $U_c \sim (x-x_0)^{-1}$, we have that $\langle u^2\rangle/(U_c)^2 \sim (x-x_0)^{m+2}$. Therefore, if m is slightly greater than -2, $\langle u^2\rangle/(U_c)^2$ (or $(\langle u^2\rangle^{0.5}/U_c)$) should grow slowly. For example, the streamwise variation of $\langle u^2\rangle^{0.5}/U_c$ for the present experiment is shown in figure 4. A power-law fit was applied to the data using $x_0 = -1.68D$, which gives a power-law exponent of 0.085 ($(m+2)/2$). This case can be observed in previous experimental data, although the reason has never been discussed in detail (perhaps due to a very slow growth). Apart from the experiments specified herein, this slow growth in turbulence intensities ($\langle u^2\rangle^{0.5}/U_c$) along the jet axis has been noted by other authors, such as Ruffin *et al.* (1994), Tong & Warhaft (1994), Amielh *et al.* (1996), Abdel-Rahman, Chakroun & Al-Fahed (1997), Xu & Antonia (2002), Fellouah *et al.* (2009), Mi, Xu & Zhou (2013) and Taub *et al.* (2013). It should be pointed out that in the aforementioned experiments (similar to the present work), the streamwise extent is limited.

The axial profile of the ratio $\langle u^2\rangle/\langle v^2\rangle$ is plotted as a function of x/D in figure 5. This ratio is approximately constant as a function of x/D with a value of 1.53. The fact that this ratio must be constant in the self-similar region was suggested previously in § 2. It is interesting to note that $\langle u^2\rangle/\langle v^2\rangle \approx 1.56$ was obtained by Hussein, Capp & George (1994) and Burattini *et al.* (2005*b*) in the self-similar region along the centreline of round jets at $Re_D = 95\,500$ and 140 000, respectively. This may suggest that the ratio $\langle u^2\rangle/\langle v^2\rangle$ (and equivalently $\langle q^2\rangle/\langle u^2\rangle$ and $\langle q^2\rangle/\langle v^2\rangle$) is not affected by

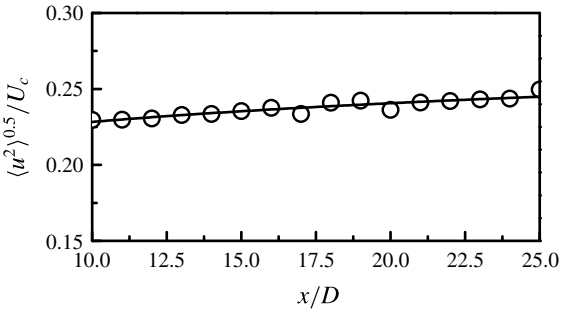

FIGURE 4. Evolution of the turbulence intensity along the centreline; the solid line is the least-squares fit to the data.

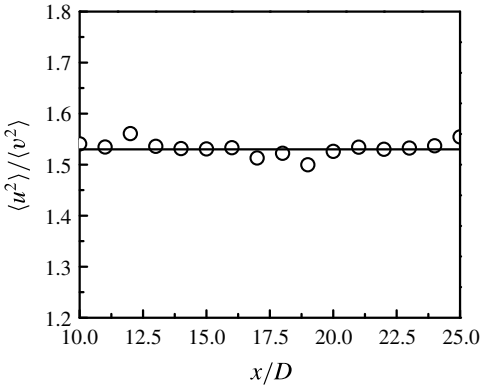

FIGURE 5. Axial profile of the ratio $\langle u^2\rangle/\langle v^2\rangle$ along the axis; the solid line is the average of the data.

the jet exit Reynolds number, at least for $Re_D \gtrsim 20\,000$, which corresponds to the onset of the mixing transition in round jets (Dimotakis 2000; Fellouah & Pollard 2010).

As discussed in § 2, the turbulent kinetic energy $\langle q^2\rangle$ and the Taylor microscale λ were shown to be the relevant scales for the similarity of all scales of flow along the jet centreline. Therefore, (2.1) and (2.4) can be rewritten as

$$f(r/\lambda) = \langle(\delta q)^2\rangle/\langle q^2\rangle \tag{4.2}$$

and

$$g(r/\lambda) = -\langle(\delta u)(\delta q)^2\rangle/(3^{-1/2}Re_\lambda^{-1}\langle q^2\rangle^{3/2}), \tag{4.3}$$

respectively. In addition, it was suggested that $\langle u^2\rangle$ and $\langle v^2\rangle$, together with λ, are relevant scales for $\langle(\delta u)^2\rangle$ and $\langle(\delta v)^2\rangle$, *viz.*

$$e(r/\lambda) = \langle(\delta u)^2\rangle/\langle u^2\rangle, \tag{4.4}$$

$$h(r/\lambda) = \langle(\delta v)^2\rangle/\langle v^2\rangle. \tag{4.5}$$

Distributions of $f(r/\lambda)$ measured at the four locations considered here ($x/D = 10$, 15, 20 and 25) are shown in figure 6. The second-order structure functions of q are found to collapse approximately at each streamwise location, which suggests that the

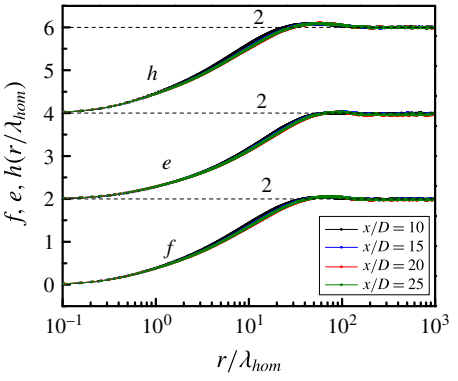

FIGURE 6. (Colour online) Distributions of f, e and h as functions of r/λ_{hom} at four axial locations $x/D = 10$, 15, 20 and 25. The structure functions have been shifted successively with respect to the lower one; each horizontal dashed line represents an offset of 2.

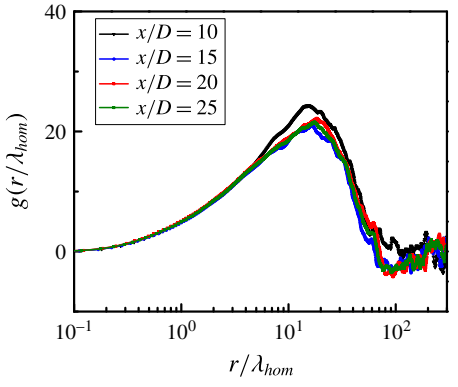

FIGURE 7. (Colour online) Distributions of $g(r/\lambda_{hom})$ at four axial locations $x/D = 10$, 15, 20 and 25.

similarity parameters found in the analysis are justified. The distributions of $e(r/\lambda)$ and $h(r/\lambda)$ are also shown in figure 6. The second-order structure functions of u and v are also found to collapse approximately using the normalisation parameters. Therefore, it can be confirmed that the suggestion that $\langle u^2 \rangle$ and $\langle v^2 \rangle$ are the relevant velocity scales for self-similarity of $\langle (\delta u)^2 \rangle$ and $\langle (\delta v)^2 \rangle$, respectively, is accurate.

The normalised third-order structure function, $g(r/\lambda)$, at locations $x/D = 10$, 15, 20 and 25 is plotted in figure 7. The collapse of $g(r/\lambda)$ is reasonable, with departures from similarity isolated to $r/\lambda \gtrsim 8$.

We now turn our attention to (2.33), which was derived as the similarity form of (1.2). The scale-by-scale budget measured at $x/D = 15$ in terms of r/λ is plotted in figure 8. The Taylor microscale λ was used to normalise r, as it was theoretically obtained to be the relevant turbulence length scale for self-preservation at all scales (§ 2). This figure demonstrates that (2.33) is adequately satisfied by the experimental data (i.e. $A + B + D + P \approx C$). Similar to Burattini *et al.* (2005*a*), at small r/λ the diffusion term B dominates, while at large r/λ the decay term D and the production term P are the dominant terms. A very good balance of all terms at very large scales confirms that the similarity forms of the production term P and inhomogeneous decay

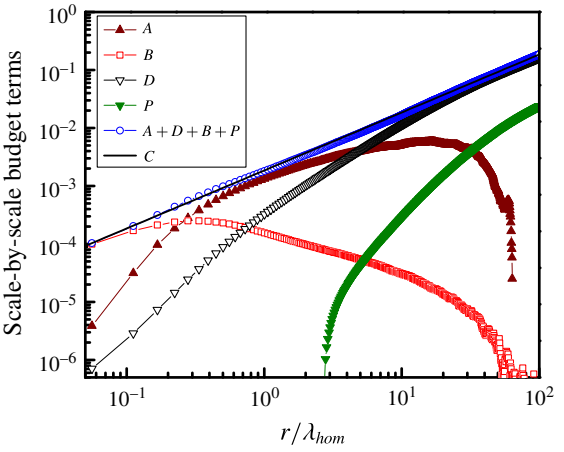

FIGURE 8. (Colour online) The terms in (2.35) at $x/D = 15$: ▲, the advection term A; □, the diffusion term B; ▽, the decay term D; ▼, the production term P; ○, the sum $A + B + D + P$. The solid black line is the dissipation term C.

term D are measured accurately. The advection term A goes to zero at both small and large separations, while its maximum is located at $r \simeq 0.8\lambda$, similar to previous observations from grid turbulence experiments and along the jet centreline (Burattini *et al.* 2005*a*). The peak value of the advection term A occurs at a value of r/λ in the vicinity of $B = D$. The production term P becomes important for $r/\lambda \gtrsim 8$, where the value of the diffusion term B begins to decrease at a higher rate with increasing r/λ. This point is very close to the value of r/λ where $A = D$.

5. Conclusion

Using an equilibrium similarity analysis, the similarity form of the transport equation of the second-order structure function was obtained along the centreline of a turbulent round jet. An important consequence of the current analysis is the derivation of forms for the decay law directly from the governing equations, rather than from classical empirical observations. It is shown that the self-similar form of the equations yields a solution such that the turbulent kinetic energy and the mean kinetic energy dissipation rate decay following power laws of the form $\langle q^2 \rangle \propto (x - x_0)^m$ and $\langle \epsilon \rangle \propto (x - x_0)^{m-2}$, respectively, along the centreline. In addition, the characteristic length scale, which was shown to be the Taylor microscale, grows as $(x - x_0)$. It is also suggested that the normalised third-order structure function can be estimated from the normalised second-order structure functions, the power-law exponent m and the decay rate constants of $\langle u^2 \rangle$ and $\langle v^2 \rangle$.

Experimental measurements were conducted at $Re_D = 50\,000$ over the range $10 \leqslant x/D \leqslant 25$ along the centreline of a round jet to validate the theoretical analysis. It was found that a power-law decay region does exist over the present range of measurements for $\langle q^2 \rangle$ with $m = -1.83$. The accuracy of this solution was confirmed using previously published data for round jets at $11\,000 \leqslant Re_D \leqslant 184\,000$ over the range $20 \leqslant x/D \leqslant 90$ ($-1.89 \leqslant m \leqslant -1.78$). Finally, the balance of all terms in (2.33), derived as a new self-similar equation for round jets, was investigated. The experimental data satisfied the relation to a very close approximation.

Acknowledgements

The authors acknowledge the financial support of the Natural Sciences and Engineering Research Council of Canada under the Discovery and RTI grant programmes. H.S. would like to thank R. J. Hearst for useful discussions.

REFERENCES

ABDEL-RAHMAN, A. A., CHAKROUN, W. & AL-FAHED, S. F. 1997 LDA measurements in the turbulent round jet. *Mech. Res. Commun.* **24**, 277–288.

AMIELH, M., DJERIDANE, T., ANSELMET, F. & FULACHIER, L. 1996 Velocity near-field of variable density turbulent jets. *Intl J. Heat Mass Transfer* **39**, 2149–2164.

ANTONIA, R. A. & BURATTINI, P. 2006 Approach to the 4/5 law in homogeneous isotropic turbuelnce. *J. Fluid Mech.* **550**, 175–184.

ANTONIA, R. A., SATYAPRAKASH, B. A. & HUSSAIN, A. K. F. M. 1980 Measurements of dissipation rate and some other characteristics of turbulent plane and circular jets. *Phys. Fluids* **23**, 695–700.

ANTONIA, R. A., SMALLEY, R. J., ZHOU, T., ANSELMET, F. & DANAILA, L. 2003 Similarity of energy structure functions in decaying homogeneous isotropic turbulence. *J. Fluid Mech.* **487**, 245–269.

BURATTINI, P. & ANTONIA, R. A. 2005 The effect of different X-wire calibration schemes on some turbulence statistics. *Exp. Fluids* **38**, 80–89.

BURATTINI, P., ANTONIA, R. A. & DANAILA, L. 2005*a* Scale-by-scale energy budget on the axis of a turbulent round jet. *J. Turbul.* **6**, 1–11.

BURATTINI, P., ANTONIA, R. A. & DANAILA, L. 2005*b* Similarity in the far field of a turbulent round jet. *Phys. Fluids* **17**, 025101.

CHAMPAGNE, F. H. 1978 The fine-scale structure of the turbulent velocity field. *J. Fluid Mech.* **86**, 67–108.

CORRSIN, S. 1963 Turbulence: experimental methods. In *Handbuch der Physik* (ed. S. Flügge & C. A. Truesdell), pp. 524–589. Springer.

DANAILA, L., ANSELMET, F. & ANTONIA, R. A. 2002 An overview of the effect of large-scale inhomogeneities on small-scale turbulence. *Phys. Fluids* **14**, 2475–2484.

DANAILA, L., ANSELMET, F., ZHOU, T. & ANTONIA, R. A. 2001 Turbulent energy scale budget equations in a fully developed channel flow. *J. Fluid Mech.* **430**, 87–109.

DIMOTAKIS, P. E. 2000 The mixing transition in turbulent flows. *J. Fluid Mech.* **409**, 69–98.

FELLOUAH, H., BALL, C. G. & POLLARD, A. 2009 Reynolds number effects within the development region of a turbulent round free jet. *Intl J. Heat Mass Transfer* **52**, 3943–3954.

FELLOUAH, H. & POLLARD, A. 2010 The velocity spectra and turbulence length scale distributions in the near to intermediate regions of a round free turbulent jet. *Phys. Fluids* **21**, 115101.

FERDMAN, E., OTUGEN, M. V. & KIM, S. 2000 Effect of initial velocity profile on the development of the round jet. *J. Propul. Power* **4**, 676–686.

FULACHIER, L. & ANTONIA, R. A. 1983 Turbulent Reynolds and Péclet number re-defined. *Intl Commun. Heat Mass Transfer* **10** (5), 435–439.

GEORGE, W. K. 1989 The self-preservation of turbulent flows and its relation to initial conditions and coherent structures. In *Advances in Turbulence* (ed. W. K. George & R. Arndt), Springer.

GEORGE, W. K. 1992 The decay of homogeneous isotropic turbulence. *Phys. Fluids* **4** (7), 1492–1509.

GEORGE, W. K. & HUSSEIN, H. J. 1991 Locally axisymmetric turbulence. *J. Fluid Mech.* **233**, 1–23.

HEARST, R. J., BUXTON, O. R. H., GANAPATHISUBRAMANI, B. & LAVOIE, P. 2012 Experimental estimation of fluctuating velocity and scalar gradients in turbulence. *Exp. Fluids* **53**, 925–942.

HINZE 1975 *Turbulence*. McGraw-Hill.

HUSSEIN, H. J., CAPP, S. & GEORGE, W. K. 1994 Velocity measurements in a high-Reynolds number, momentum-conserving, axisymmetric, turbulent jet. *J. Fluid Mech.* **258**, 31–75.

LAVOIE, P., BURATTINI, P., DJENIDI, P. & ANTONIA, R. A. 2005 Effect of initial conditions on decaying grid turbulence at low R_λ. *Exp. Fluids* **39** (5), 865–874.

LUMLEY, J. L. 1965 Interpretation of time spectra measured in high-intensity shear flows. *Phys. Fluids* **8**, 1056–1062.

MALMSTROM, T. G., KIRKPATRICK, A. T., CHRISTENSEN, B. & KNAPPMILLER, K. D. 1997 Centreline velocity decay measurements in low-velocity axisymmetric jet. *J. Fluid Mech.* **246**, 363–377.

MI, J., XU, M. & ZHOU, T. 2013 Reynolds number influence on statistical behaviors of turbulence in a circular free jet. *Phys. Fluids* **25**, 075101.

PANCHAPAKESAN, N. R. & LUMLEY, J. L. 1993 Turbulence measurements in axisymmetric jets of air and helium. Part 1. Air jet. *J. Fluid Mech.* **246**, 197–223.

POLLARD, A. & UDDIN, M. 2007 Self-similarity of coflowing jets: the virtual origin. *Phys. Fluids* **19**, 068103.

POPE, S. B. 2000 *Turbulent Flows*. Cambridge University Press.

QUINN, W. R. 2006 Upstream nozzle shaping effects on near field flow in round turbulent free jets. *Eur. J. Mech. (B/Fluids)* **25**, 279–301.

RUFFIN, E., SCHIESTEL, R., ANSELMET, F., AMIELH, M. & FULACHIER, L. 1994 Investigation of characteristic scales in variable density turbulent jets using a secondorder model. *Phys. Fluids* **6**, 2785–2799.

SADEGHI, H., LAVOIE, P. & POLLARD, A. 2014 The effect of Reynolds number on the scaling range along the centreline of a round turbulent jet. *J. Turbul.* **15**, 335–349.

SADEGHI, H. & POLLARD, A. 2012 Effects of passive control rings positioned in the shear layer and potential core of a turbulent round jet. *Phys. Fluids* **24**, 115103.

TAUB, G. N., LEE, H., BALACHANDAR, S. & SHERIF, S. A. 2013 A direct numerical simulation study of higher order statistics in a turbulent round jet. *Phys. Fluids* **25**, 115102.

TENNEKES, H. & LUMLEY, J. L. 1972 *A First Course in Turbulence*. MIT Press.

TONG, C. & WARHAFT, Z. 1994 Turbulence suppression in a jet by means of a fine ring. *Phys. Fluids* **6**, 328–333.

WEISGRABER, T. H. & LIEPMAN, D. 1998 Turbulent structure during transition to self-similarity in a round jet. *Exp. Fluids* **24**, 210–224.

WYGNANSKI, I. & FIEDLER, H. 1969 Some measurements in the self-preserving jet. *J. Fluid Mech.* **38**, 577–612.

XU, G. & ANTONIA, R. A. 2002 Effect of different initial conditions on a turbulent round free jet. *Exp. Fluids* **33**, 677–683.

XU, M., POLLARD, A., MI, J., SECRETAIN, F. & SADEGHI, H. 2013 Effects of Reynolds number on some properties of a turbulent jet from a long square pipe. *Phys. Fluids* **25**, 035102.